Ho centres in ZnS in the 3+ and 2+ state studied by optical and electron paramagnetic

resonance spectroscopy

Ho centres in ZnS in the 3+ and 2+ state studied by optical and electron paramagnetic resonance spectroscopy

R Boyn, St Müller, J Dziesiaty and H Zimmermann

Humboldt-Universität zu Berlin, Institut für Physik, Berlin, Germany

Abstract. Ho centres in mixed-polytype ZnS crystals codoped with Ag are studied by measuring polarized site-selective photoluminescence and photoluminescence excitation spectra as well as by EPR spectroscopy. The optical data give evidence of Ho in the charge state 3+ ($4f^{10}$), while in the EPR measurements, which are performed under illumination in the interband range, centres in the 2+ state ($4d^{11}$) are detected.

From a crystal-field analysis we conclude that the dominant centres seen in the two kinds of experiment are identical with respect to the atomic configuration, apart from small nearest-neighbour relaxation effects which accompany the change of the charge state. The crystal field is found to have approximately cubic symmetry, with a small trigonal field component, whose axis is parallel to the $[111]_w$ direction. Our data indicate that the Ho occupies zincblende-type interstitial sites with four metallic ions as nearest neighbours, most probably Ag substituting for Zn ions.

The Ho^{2+} ground state involved in the charge transfer process is thought to lie close to the bottom of the conduction band: this explains the optical behaviour observed in our experiments.

1. Introduction

Recently there has been increasing interest in rare-earth- (RE-) doped semiconductors due to the possibility of employing 4f–4f optical transitions in light-emitting semiconductor devices [1]. RE-doped materials exhibiting a large number of 4f–4f emission bands in the visible spectral range, such as $ZnS:Ho^{3+}$ [2], deserve special attention.

One of the most important characteristics affecting the luminescent properties, including the emission efficiency, is the charge state in which the RE ions occur in the crystal lattice, which has been re-emphasized, for example, by recent work on RE-doped III–V semiconductors [3]. REs in the II–VI compounds have been found to exist mostly in the charge state 3+. However, in a number of cases the occurrence of the 2+ state (which involves an additional electron in the 4f shell) has been concluded from EPR experiments (see, e.g., the review [4]). In some of these experiments illumination-induced changes of the charge state between 3+ and 2+ have been demonstrated [5, 6]. Obviously, the observability of the 2+ state depends on whether the 2+ ground level is located below or above the conduction band edge.

Theoretical studies [7] indicate that deep-lying 2+ levels are to be expected mainly in the middle and at the end of the lanthanide series. This is confirmed by the available experimental data, which refer to Eu, Er, Tm, and Yb impurities in various II–VI hosts [4, 6, 8, 9]. In addition to the type of RE ion, the location of the 2+ level should also depend on the host material [7] and on the type of site on which the ion is incorporated into the lattice.

To get reliable data on both the charge state and the kind of incorporation of the RE ions, it is important to combine EPR with site-selective optical studies. For RE-doped semiconductors this combination has been used only in very few cases. In the present paper we report on such studies of Ho centres in bulk ZnS:Ho crystals. Luminescence spectra of this system have only been investigated in old work using powder samples and non-selective excitation [2], while corresponding EPR data are completely missing. In agreement with [2], our optical experiments give evidence of the charge state Ho^{3+} ($4f^{10}$). This charge state is not detected in EPR, as is the usual situation for non-Kramers ions (for exceptions see [8, 9]). However, illumination in the interband range leads to a partial conversion to the Ho^{2+} ($4f^{11}$) state which we see in the EPR spectrum.

We find that a single type of centre is dominant in most of the optical 4f–4f spectra as well as in the EPR spectra. From the agreement with respect to symmetry and the results of a crystal-field analysis we infer that we are dealing with the same species in the two experiments and draw conclusions as to the structure of those centres.

2. The samples

The ZnS crystals were grown by sublimation at about 1100 °C (growth time three months). The starting material was ZnS powder with an admixture of Ho metal (about 0.1 molar per cent) and Ag_2S (about 0.05 molar per cent). The Ag_2S was added in view of the experience that codoping with acceptor-type impurities (i) facilitates the incorporation of RE ions and (ii) may reduce the number of centres by binding those ions into very few RE–acceptor complexes [4]. Platelet-shaped crystals with a thickness of about 1 mm were selected from the sublimate. Our EPR and optical data indicate that the crystals have mixed-polytype character with a definite hexagonal axis ($[111]_w$ axis) lying in the large faces of our samples and parallel to the striations visible on these faces.

The total Ho concentration was determined by RBS analysis to be $(3 \text{ to } 5) \times 10^{19}$ cm^{-3}. The concentration of the Ho centre A, which is studied in detail in this work, was estimated to be some 10^{18} cm^{-3} from 4f–4f absorption measurements.
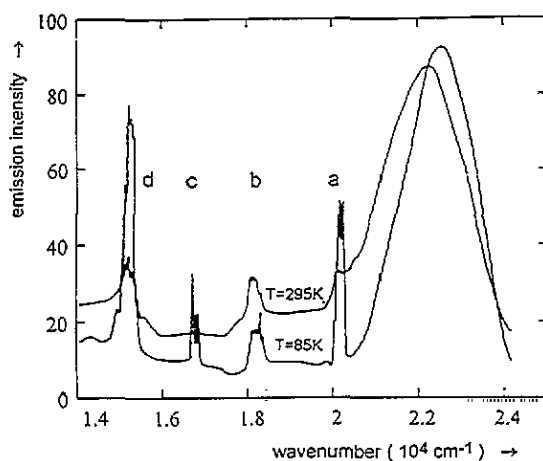

Figure 1. Nonselective PL spectra measured with 365 nm excitation, including four Ho^{3+} 4f–4f intermultiplet transitions (bands a to d, see the text for assignments). The spectra have been corrected for the spectral sensitivity of the apparatus.
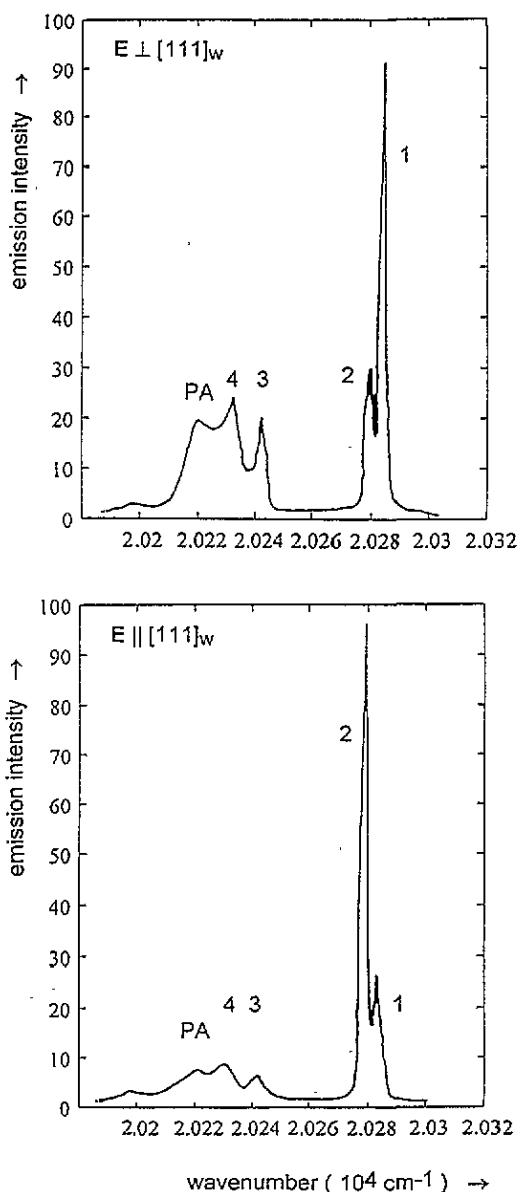
Figure 2. The polarized site-selective Ho^{3+} $^5F_3 \to {}^5I_8$ PL spectrum measured with dye-laser excitation in the $21\,907$ cm^{-1} line (figure 4) at 27 K. The numbers at the lines refer to the assignments given in figure 6. E is the electric field vector of the radiation.

3. Photoluminescence and photoluminescence excitation spectra

In figure 1 we show, for two temperatures, the photoluminescence (PL) spectrum in the visible range excited by the 365 nm radiation of a high-pressure mercury lamp. This spectrum exhibits four groups of lines (a to d), which are due to Ho^{3+} 4f–4f transition, *viz* $^5F_3 \to {}^5I_8$ (a), $^5S_2 \to {}^5I_8$ (b), $^5G_4 \to {}^5I_6$ (c), $^5F_5 \to {}^5I_8$ (d), and $^5F_3 \to {}^5I_7$ (d). Transitions of similar energies could be excluded by measuring excitation spectra (broad-

band as well as 4f–4f excitation spectra). These assignments essentially agree with those given in [2]. In addition to the 4f–4f luminescence, figure 1 shows a broad emission band centred about 22 000 to 23 000 cm^{-1}, which is probably the 'blue Ag band' [10] related to our Ag codopant.

Site-selective 4f–4f emission measurements were performed at liquid neon temperature using a dye laser pumped by a pulsed nitrogen laser. It was found that the 4f–4f *excitation spectrum* (see below) is dominated by a single type of centre (site). The selective spectra of this centre (to be referred to as centre A) were studied in detail, and results will be given in the following. It should be noted that a considerable number of additional centres contribute to the PL spectrum measured with nonselective excitation as in figure 1. Surprisingly, the contribution of centre A to this spectrum is relatively small, which may indicate the absence of 'external excited states' [4, 11] in the energy range of the 365 nm excitation. An RE centre with similar behaviour has been recently detected in GaAs:Er [12].

Figures 2 and 3 show the selective PL spectra of centre A due to $^5F_3 \rightarrow ^5I_8$ (band a) and $^5F_3 \rightarrow ^5I_7$ (band d) transitions, respectively. (It follows from the crystal-field analysis to be presented below that only the latter transitions contribute to the emission of this centre in the d-band range.) The spectra are strongly polarized with respect to the $[111]_w$ crystal axis. This result shows that the centre symmetry is not cubic. Since the polarization was found to be independent of the polarization of the exciting dye-laser radiation, we conclude that we are not concerned with several equivalent axial complexes having different orientations. Rather, we should be dealing with centres whose symmetry axes are parallel to $[111]_w$ for each individual. A more detailed discussion of the type of centre will be given in section 5.

In figure 4 we present the 4f–4f excitation spectrum for one line from figure 3, in the range of the $^5I_8 \rightarrow ^3K_8, ^5G_6$ transitions. Exactly the same spectrum was observed for several other emission lines in figures 2 and 3. The excitation spectrum is dominated by the line at 21 907 cm^{-1}. We think that this line is due to $^5I_8 \rightarrow ^5G_6$ transitions, which are known to be hypersensitive and to have an especially large oscillator strength [13].

4. EPR spectra

EPR spectra were studied at 3.5 K in the X-band ($h\nu = 0.3097$ cm^{-1}). The dominant signal (figure 5), which appeared under illumination with interband light from a high-pressure mercury lamp, will be discussed in detail in the following.

Natural holmium consists of a single isotope with a nuclear spin $I = 7/2$. For a ground-state doublet of an axial centre, the spin Hamiltonian is

$$H = g_{\|}\beta B_z S_z + g_{\perp}\beta(B_x S_x + B_y S_y) + A_{\|}S_z I_z + A_{\perp}(S_x I_x + S_y I_y) + g_N \beta_N \boldsymbol{B} \cdot \boldsymbol{I} \tag{1}$$

where the small term $g_N \beta_N \boldsymbol{B} \cdot \boldsymbol{I}$ may be neglected. All the symbols have the usual meaning.

Because of the large hyperfine splitting ($4A \geqslant h\nu$), only two resonance lines are observed *for all directions* of $\boldsymbol{B}$ in the $(110)_w$ plane (figure 5). If the symmetry axes of all the centres are parallel to $[111]_w$, the eigenvalues of (1) for $\boldsymbol{B}\|[111]_w$ and $\boldsymbol{B}\perp[111]_w$ are given by the well-known Breit–Rabi formula

$$\varepsilon_{\pm}(m) = -(A/4) \pm (1/2)[(g\beta B_0)^2 + 2mAg\beta B_0 + I(I+1)A^2]^{1/2} \tag{2}$$

where $m = m_S + m_I$, and the subscripts $\|$ and $\perp$ have been omitted. B_0 is the magnitude of the resonance field strength. The observed transitions can be described on the basis of (2).

Strong transitions are between the levels $\varepsilon_+(m)$ and $\varepsilon_-(m-1)$. Two kinds of such transitions are found at low fields: (i) with a change in the electronic spin quantum number
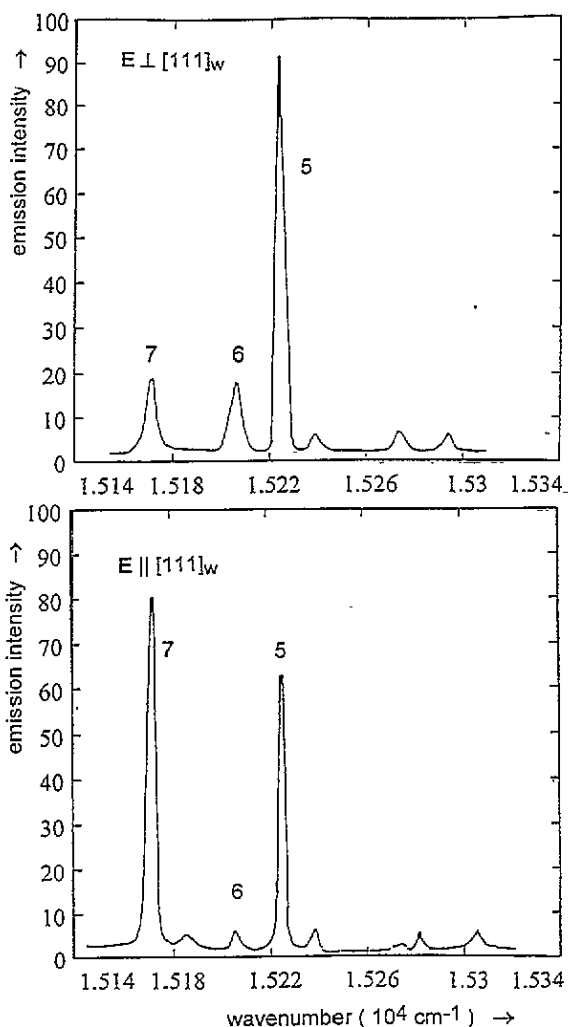
Figure 3. The polarized site-selective Ho^{3+} $^5F_3 \rightarrow {}^5I_7$ PL spectrum measured with dye-laser excitation in the 20907 cm^{-1} line (figure 4) at 27 K. The numbers at the lines refer to the assignments given in figure 6. The additional low-intensity lines at high energies (not labelled) are probably due to a different centre (to different centres) not completely eliminated by the monoenergetic excitation. *E* is the electric field vector of the radiation.

only ($m_S = -1/2 \rightarrow +1/2$, $m_I = -7/2$; $m = -4 \rightarrow -3$) and (ii) a change in the nuclear quantum number only ($m_S = -1/2$, $m_I = -7/2 \rightarrow -5/2$; $m = -4 \rightarrow -3$) (table 1).

The data can be fitted to (2) using $g_\parallel = 4.47 \pm 0.005$, $g_\perp = 6.0 \pm 0.005$, $A_\parallel = 0.098 \pm 0.001$ cm^{-1}, and $A_\perp = 0.120 \pm 0.001$ cm^{-1}. The fitted angular dependence shows only insignificant deviations from the experimental dependence presented in figure 5. The linewidth of the transitions is about 0.001 T for $g_\parallel$ and 0.002 T for $g_\perp$.

These results show that the signal is due to a Ho centre with axial symmetry, the symmetry axis being parallel to the [111]$_w$ axis, just as found for the optical centre A.
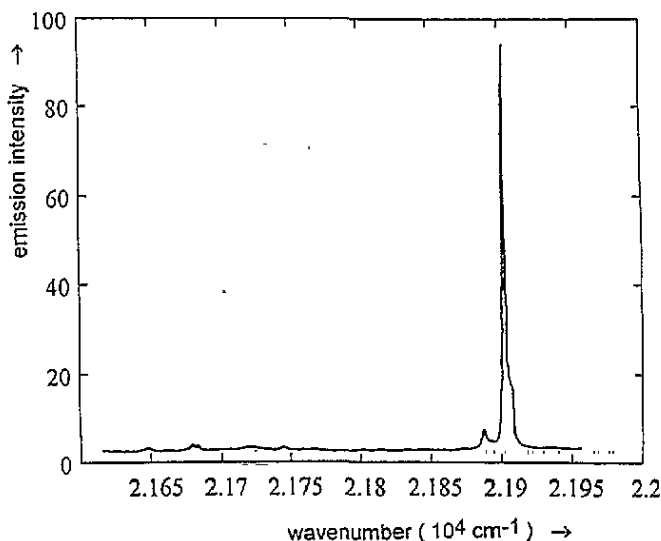
Figure 4. The site-selective PLE spectrum measured in the $^5I_8 \rightarrow$ $^3K_8$, $^5G_6$ range at 27 K, monitoring the 15 224 cm^{-1} Ho^{3+} $^5F_3 \rightarrow$ $^5I_7$ emission line (figure 3, transition No 5).
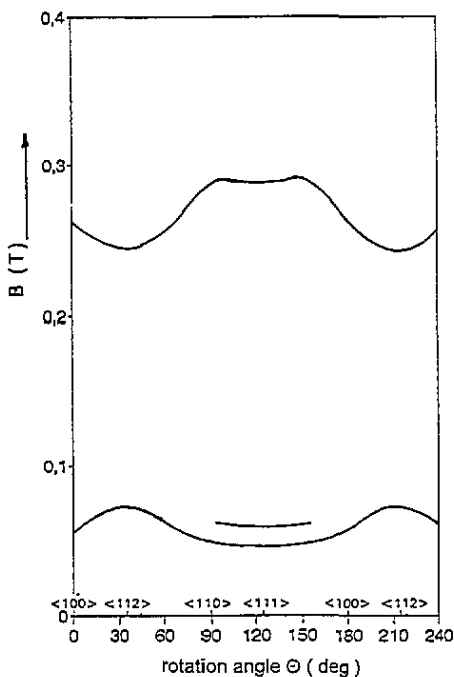

Figure 5. The angular dependence of the EPR signals due to the centres investigated, measured by varying the magnetic field direction in the (111)$_w$ plane (X-band, $T = 3.3$ K). It is an open question whether the line about 0.06 T, which is observed only at angles around 120°, originates from the centre discussed in this paper.

5. Crystal-field analysis and discussion of the type of centres

As a starting point of our discussion we shall use the level diagrams of Lea, Leask, and Wolf (LLW) [14] referring to cubic symmetry. For noncubic centres this procedure (which

Table 1. Observed EPR transitions in Ho^{2+} centres in ZnS.

Observed field strength (T)	Transition (high-field notation)
$B \parallel [111]_w$	
0.2890	$|1/2, -7/2\rangle \rightarrow |-1/2, -7/2\rangle$
0.0480	$|-1/2, -7/2\rangle \rightarrow |-1/2, -5/2\rangle$
$B \perp [111]_w$	
0.2450	$|1/2, -7/2\rangle \rightarrow |-1/2, -7/2\rangle$
0.0740	$|-1/2, -7/2\rangle \rightarrow |-1/2, -5/2\rangle$

has been employed in earlier work on similar systems [15–17]) should be justified if the noncubic crystal-field component is weak. That this condition is fulfilled for the present centres is demonstrated by the following analysis.

5.1. Charge state 3+

A crystal-field analysis was performed for the multiplets involved in the $^5F_3 \rightarrow {}^5I_8$ and $^5F_3 \rightarrow {}^5I_7$ optical transitions aiming at a quantitative description of the spectra in figures 2 and 3. This analysis was based on the $J = 3$, $J = 7$, and $J = 8$ LLW diagrams. The effect of a small crystal-field component of trigonal symmetry (symmetry axis parallel $[111]_w$), which adds to the dominant cubic contribution, was taken into account only qualitatively, in order to explain the presence of small additional line splittings and—on the basis of selection rules—the polarization behaviour found in experiment. Since $\Delta J = 5$ and 4, respectively, for the present intermultiplet transitions, these should have pure electric dipole character [13]; so electric dipole selection rules were considered in our analysis.

When trying to arrive at a quantitative fit, difficulties were met which obviously result (i) from level shifts produced, in addition to splittings, by the trigonal field and (ii) from effects of electron–phonon coupling familiar for RE centres in ZnS [18]. A systematic variation of the cubic crystal-field parameters $A_4\langle r^4\rangle$ and $A_6\langle r^6\rangle$ using Stevens coefficient from [19] showed that a reasonable description of the experimental data could only be achieved for positive $A_4\langle r^4\rangle$ and negative $A_6\langle r^6\rangle$. In figure 6 we present a level scheme calculated for $A_4\langle r^4\rangle = 137$ cm^{-1} and $A_6\langle r^6\rangle = -6.4$ cm^{-1} together with an assignment of the transitions found in experiment.

In determining the crystal-field parameters we took into account that for RE centres transitions to higher Stark components of a given multiplet tend to have small intensity and are frequency unobservable (e.g. [12, 18, 20]). This has been related to a 'dissolution' [18] of the transitions to the higher components in phonon sidebands of the transitions to lower components, hence the former transitions are thought to contribute only to a rather smooth background. Phonon-assisted transitions seem also to be responsible for the broad line at 20 221 cm^{-1} in the $^5F_3 \rightarrow {}^5I_8$ spectrum (figure 2, labelled PA), which is not accounted for by the crystal-field model. These transitions should be related to the zero-phonon transition 1 and should involve phonons in the TA range, probably modified by the large mass of the Ho ion.

The measured spectra in figures 2 and 3 deviate from the crystal-field model in the respect that the model predicts complete polarization in all cases in which trigonal splitting components are resolved, while only partial polarization is found in experiment. In our view, this deviation is related to contributions of light multiply reflected within the samples.
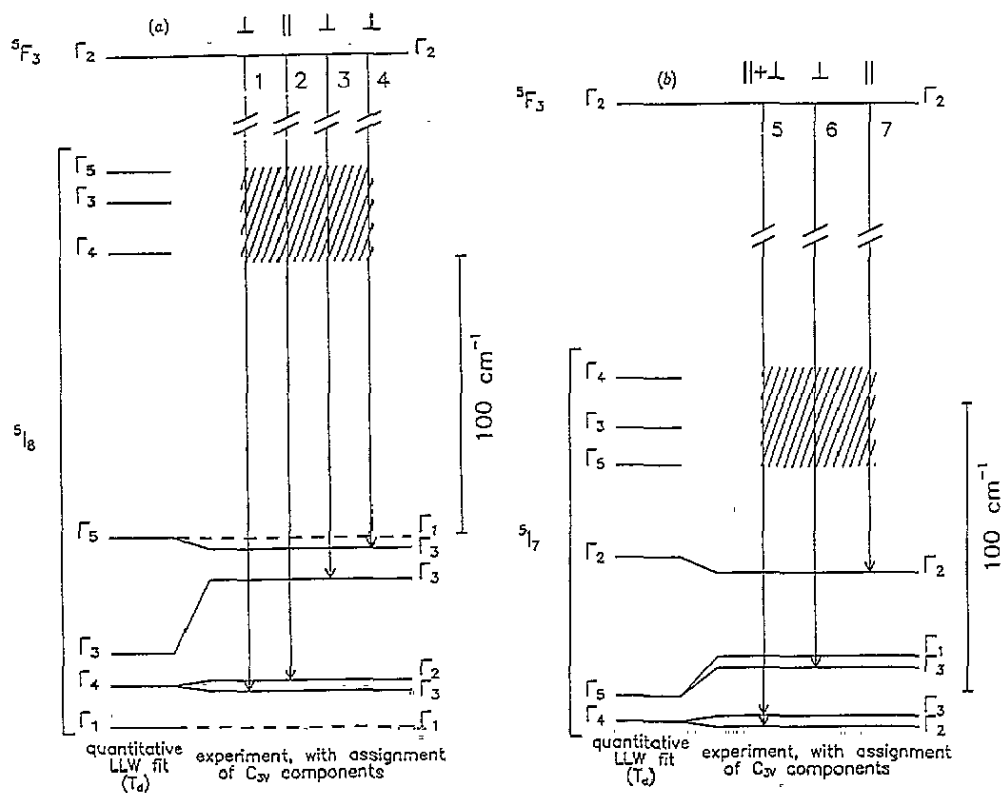
Figure 6. (a) Assignment of the observed Ho^{3+} $^5F_3$ → $^5I_8$ emission lines of centre A to electric dipole transitions between trigonal (C_{3v}) crystal-field components (right) and comparison with a cubic crystal-field calculation (T_d symmetry) using the parameters $A_4\langle r^4\rangle = 137$ cm^{-1}, $A_6\langle r^6\rangle = -6.4$ cm^{-1} (left). The transitions are labelled to correlate them with the lines in the spectra in figure 2. Levels not observed in experiment because of selection rules and phonon effects (see the text) are indicated by dashed lines and hatched areas, respectively. Only the lowest Stark component of the $^5F_3$ multiplet is shown, its separation from the second lowest (Γ_5) component being 61 cm^{-1} according to the LLW fit. (b) As (a), but for the $^5F_3$ → $^5I_7$ emission lines of centre A, to be correlated with the spectra in figure 3.

Not included in figure 6 is the $^5G_6$ multiplet, which is thought to be the final multiplet for the dominant 4f–4f excitation transitions (figure 4). The 21 907 cm^{-1} line should derive from electric dipole transitions between the Γ_1 ($^5I_8$) state and one of the Γ_5 components [14] of $^5G_6$.

The presence of a trigonal crystal-field component shows that the centres are located in hexagonal regions of our mixed-polytype crystals. Information on the nature of the centres can be obtained *from the signs* of the parameters $A_4\langle r^4\rangle$ and $A_6\langle r^6\rangle$ by comparison with a point-ion model, including, as usual, nearest-neighbour (nn) ions for substitutional sites and both nearest and next-nearest neighbours (nnn) for interstitial sites (see the appendix). This gives an argument against Zn site occupation, for which $A_4\langle r^4\rangle$ should be negative. Considering now interstitial site occupation, we have to take into account that of the four types of interstices occurring in mixed-polytype ZnS (two zincblende-type and two wurtzite-type [4]) the wurtzite-type sites can also be excluded because the crystal field exhibits serious deviations from cubic symmetry [21]. Agreement with the observed signs of $A_4\langle r^4\rangle$ and
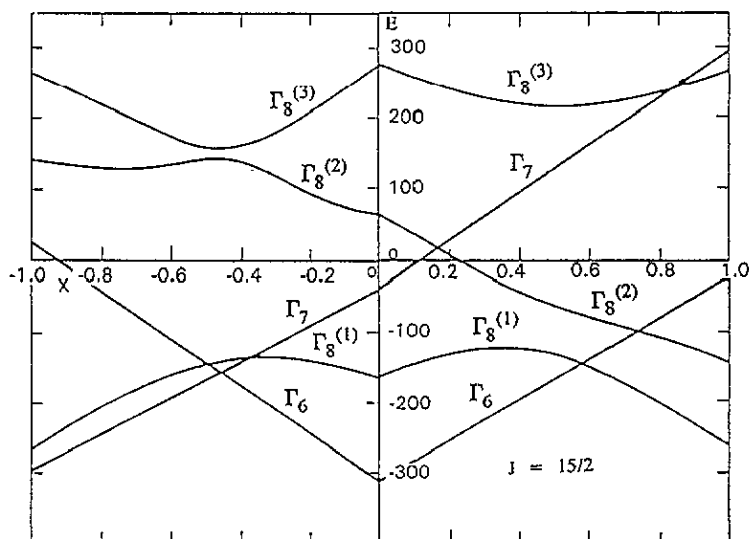
Figure 7. The LLW diagram [14] used for discussing the splitting of the Ho^{2+} $^4I_{15/2}$ level due to a cubic (tetrahedral) crystal field.

$A_6\langle r^6\rangle$ is obtained only for the zincblende-type sites with four tetrahedrally arranged nn metal ions and six octahedrally arranged nnn S ions. The origin of the trigonal crystal-field component will be discussed later.

Next we present evidence that centre A is responsible also for the Ho^{2+} EPR signals analysed in section 4.

5.2. Charge state 2+

Divalent holmium is isoelectronic to trivalent erbium; so the ground multiplet is $^4I_{15/2}$. The $J = 15/2$ LLW diagram [14] (figure 7) shows that in a cubic crystal field this multiplet involves five components. According to the experience obtained for Er^{3+} and Ho^{2+} in tetrahedron- and cube-type coordination [15–17, 22, 23], and using point-ion considerations as in section 5.1, we expect that the lowest component studied in EPR is Γ_6 or Γ_7 in the case of metal-site occupation, and for the occupation of the zincblende-type interstices with a nonmetal nn tetrahedron. For the interstitial sites having four metallic nn ions the cubic ground levels should be $\Gamma_8^{(3)}$ or $\Gamma_8^{(1)}$ (figure 7).

For the Kramers doublets Γ_6 and Γ_7, a small trigonal crystal field with symmetry-axis parallel to $[111]_w$ will introduce an anisotropy of the g-factors. If this field is small, the average values $(1/3)(g_\parallel + 2g_\perp)$ are expected to be close to the cubic values $2\Lambda\langle\Gamma_i|J_z|\Gamma_i\rangle$ ($\Lambda = 6/5$ Landé factor) [17], which should be 6.8 and 6.0 for $i = 6$ and $i = 7$, respectively. For the present centres the average value is 5.49 (section 4); so it is improbable that Γ_6 and Γ_7 states are involved. On the other hand, we get reasonable agreement with the experimental data on the basis of Γ_8 states modified by the trigonal field: such a field will split the Γ_8 levels into two Kramers doublets. If this splitting is small against the splitting due to the cubic field, one can still use the eigenvectors as given by LLW [14]. Denoting the eigenvectors, as usual, by $|\Gamma_8, \pm 1/2\rangle$ and $|\Gamma_8, \pm 3/2\rangle$ one obtains for the principal g-values of the active doublet [24]

$$|g_\parallel| = \Lambda(P - Q) \qquad |g_\perp| = \Lambda(P + Q) \tag{3}$$

where $P = \langle \Gamma_8, 3/2 | J_z | \Gamma_8, 3/2 \rangle$ and $Q = \langle \Gamma_8, 1/2 | J_z | \Gamma_8, 1/2 \rangle$ (quantization along $\langle 100 \rangle$).

Since we are dealing with more than one Γ_8 level, the g-factors depend upon the LLW parameter x. Figure 8 presents the x-dependence for $\Gamma_8^{(1)}$ and $\Gamma_8^{(3)}$ calculated on the basis of (3). Satisfactory agreement with experiment is obtained for $\Gamma_8^{(1)}$ and $x = 0.6$, yielding $g_\parallel = 4.8$ and $g_\perp = 6.8$. The deviations may be related to mixing with the neighbouring Γ_6 state. Hence we should be concerned with zincblende-type interstitial sites having four metallic nn ions, as in the case of the optical centre A. Using Stevens coefficients for Er^{3+} from [14], $x = 0.6$ implies a ratio $\lambda \equiv A_6 \langle r^6 \rangle / A_4 \langle r^4 \rangle$ of 0.062, i.e. positive values of both $A_4 \langle r^4 \rangle$ and $A_6 \langle r^6 \rangle$. On the other hand, a λ-value of -0.047 is obtained for centre A from the analysis in section 5.1.

Assuming that we see the same centres in our optical and EPR experiments, the difference of the λ-values has to be attributed to a change in the crystal field which is *a secondary consequence of the $Ho^{3+} \leftrightarrow Ho^{2+}$ process. In our view, such an interpretation* can be given in a very natural manner: we think that the main effect comes from the change in the nn atomic relaxation induced by the change of the Ho ionic radius. On going from Ho^{3+} to Ho^{2+} we expect an additional outward relaxation of the four metallic nn ions, which should decrease the magnitude of their contribution to the crystal-field parameters. Since the contributions of nn and nnn ions to $A_6 \langle r^6 \rangle$ have opposite signs and comparable magnitude (see the appendix), the decrease in the magnitude of the former could lead to a change of the sign of that parameter and, consequently, a change in the sign of λ.

5.3. The origin of the trigonal crystal field

As we have argued, our optical and EPR data should refer to the same type of centre, which involves Ho and zincblende-type interstitial sites having four metallic nn ions. There are several possibilities for the origin of the trigonal crystal-field component.

One possibility would be isolated interstitial Ho ions, i.e. ions not forming a complex with other defects. In this case the trigonal field would have to be attributed to the *configuration of the neighbouring Zn and S ions deviating from the cubic situation.*

However, in view of our Ag_2S codoping, it is natural to assume that the positive excess charge of the Ho interstitial is locally compensated, to some extent, by acceptor-type Ag impurities substituting for nn Zn ions. There are three variants of such centres involving a trigonal field parallel to $[111]_w$: (i) only the Zn ion in the $[111]_w$ direction is replaced; (ii) the three Zn ions away from the $[111]_w$ direction are replaced; (iii) all four Zn ions are substituted by Ag ions. While in cases (i) and (ii) the main contribution to the trigonal field should come from the changed identity of nn ions, only the (probably much smaller) effect of the dilation/compression, parallel to $[111]_w$, of the nn tetrahedron and nnn octahedron will be operative in case (iii).

In our view, case (iii) is the most probable one, because of the smallness of the trigonal level-splittings seen in our optical spectra (figures 2 to 4, figure 6). It should be noted that an analogous kind of centre has been identified in early optical and EPR work on ZnSe:Er, Cu [22]. In that (exactly cubic) system, all four nn Zn ions are thought to be substituted by acceptor-type Cu impurities. Remarkably, in that case the effect on $A_6 \langle r^6 \rangle$ of the nn tetrahedron is also found to be smaller than that of the nnn octahedron (positive value of our parameter λ).

These results are consistent with the general observation that strong group-I codoping favours the incorporation of REs on the type of interstitial site considered [4, 16] (or on wurtzite-type interstitial sites [21]) relative to substitutional incorporation.
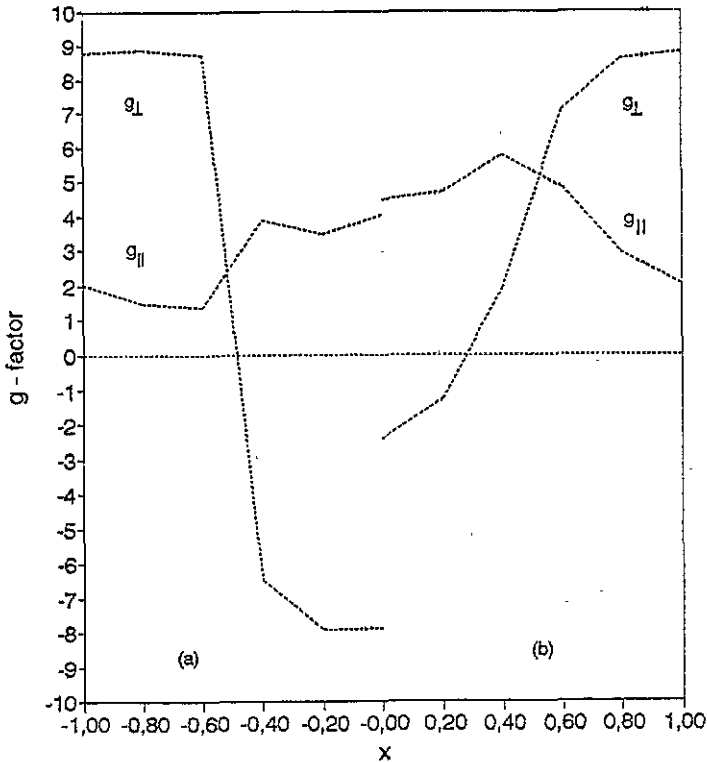
Figure 8. g-values for $\Gamma_8^{(1)}$ ($^4I_{15/2}$) and $\Gamma_8^{(3)}$ ($^4I_{15/2}$) states (figure 7) in the presence of a small trigonal crystal-field component, calculated as a function of the LLW parameter x. The labels $\parallel$ and $\perp$ refer to the direction of the trigonal axis.

6. Concluding remarks

We have observed and analysed Ho centres in the 3+ and 2+ charge state, by optical and EPR spectroscopy. We argue that we are concerned with the same centres in the two cases which involve the occupation of zincblende-type interstitial sites having four metallic ions as nearest neighbours, most probably Ag substituted for Zn ions.

The differences of the crystal fields found for Ho^{3+} and Ho^{2+} are thought to arise from the nn ionic relaxation which is due to the difference in the respective ionic radii. The presence of a small crystal-field component should be due to the slight dilation/compression along the $[111]_w$ direction, of the nn tetrahedron and the nnn octahedron.

Since, in our case, the Ho^{2+} EPR signal appears only under illumination, the corresponding ground level should lie in the band gap. This level should have donor character and should be compensated by acceptors in the dark state. From the general trends predicted for 4f ground-state positions [7] we expect to find that the Ho^{2+} level is rather close to the conduction band edge. This is supported by the result that the EPR spectrum could be detected under illumination in the interband range, but was found to be quenched by exposing the samples to radiation in the red and infrared regions. This implies that Ho^{3+} cannot be transformed to Ho^{2+} by low-energy transitions from the valence band, but that the transformation occurs through the capture of conduction electrons which are generated by the interband light. The quenching can be attributed to the optical release of

electrons from the 2+ levels to the conduction band.

Moreover, such a level position can explain the absence of 4f–4f emission due to Ho^{2+}; this emission is obviously quenched by autoionization of the excited Ho^{2+} states into the conduction band.

Acknowledgments

Appendix

For the reader's convenience we present here expressions for the crystal-field parameters emerging from a point-ion model in the case of cubic symmetry, which we have been using to discuss the signs of our experimental values. Strictly speaking, these expressions refer to substitutional and interstitial centres in zincblende-structure crystals. Including, as usual [4], contributions of nn ions in the substitutional case, and contributions of both nn and nnn ions in the interstitial case, we have

$$A_4\langle r^4\rangle = (7Z_1e^2/36R_1^5)\langle r^4\rangle \tag{A1}$$
$$A_6\langle r^6\rangle = -(Z_1e^2/18R_1^7)\langle r^6\rangle \tag{A2}$$

for substitutional centres and

$$A_4\langle r^4\rangle = [(7Z_1e^2/36R_1^5) - (7Z_2e^2/16R_2^5)]\langle r^4\rangle \tag{A3}$$
$$A_6\langle r^6\rangle = [-(Z_1e^2/18R_1^7) - (3Z_2e^2/64R_2^7)]\langle r^6\rangle \tag{A4}$$

for interstitial centres. Z_1e and R_1 are the charge and the distance, respectively, of the nn ions, and Z_2e and R_2 are the charge and the distance, respectively, of the nnn ions.

These expressions can be used, as 'cubic approximations', for substitutional centres and zincblende-type interstitial centres in mixed-polytype ZnS crystals as studied in the present paper, if the trigonal crystal-field effects are small. Such effects arise, e.g., from the small dilations/compressions parallel to the $[111]_w$ direction, of the tetrahedra and octahedra, and also from the configurations of more distant neighbours, as have been discussed for the substitutional case, in relation to transition metal impurities, in [25].

In considering the effect of ionic relaxation induced by the $Ho^{3+} \leftrightarrow Ho^{2+}$ recharging process (section 5), we are referring to the decrease of the first term in the square brackets in (A4), whose sign is opposite to that of the second term.

References

[1] *Proc. Symp. on Rare Earth Doped Semiconductors (San Francisco, CA 1993), Mater. Res. Soc. Proc.* vol 301 (Pittsburgh, PA: Materials Research Society)
[2] Ibuki S and Langer D 1964 *J. Chem. Phys.* **40** 796
[3] Klein P B, Moore F G and Dietrich H B 1991 *Appl. Phys. Lett.* **58** 502
[4] Boyn R 1988 *Phys. Status Solidi* b **148** 11
[5] Godlewski M and Hommel D 1986 *Phys. Status Solidi* a **95** 261
[6] Swiatek K, Godlewski M 1990 *Phys. Rev.* B **42** 3628
[7] Delerue C and Lannoo M 1991 *Phys. Rev. Lett.* **67** 3006
[8] Müller St and Dziesiaty J 1994 *Phys. Status Solidi* b **184** 483

[9] Dziesiaty J, Müller St, Boyn R, Buhrow Th, Klimakow A and Kreissl J 1995 *J. Phys.: Condens. Matter* **7** 4271

[10] Era K, Shionoya S and Washizawa Y 1968 *J. Phys. Chem. Solids* **29** 1827

[11] Zimmermann H and Boyn R 1986 *Phys. Status Solidi* b **135** 379

[12] Takahei K and Taguchi A 1995 *J. Appl. Phys.* **77** 1735

[13] Peacock R D 1975 *Structure Bonding* **22** 83

[14] Lea K R, Leask M J M and Wolf W P 1962 *J. Phys. Chem. Solids* **23** 1381

[15] Watts R K and Holton W C 1968 *Phys. Rev.* **173** 417

[16] Crowder B L, Title R S and Pettit G D 1969 *Phys. Rev.* **181** 567

[17] Lewis H R and Sabisky E S 1963 *Phys. Rev.* **130** 1370

[18] Boyn R and Zimmermann H 1987 *Phys. Status Solidi* b **140** 163

[19] Rajnak K and Krupke W F 1967 *J. Chem. Phys.* **46** 3532

[20] Przybylinska H, Enzenhofer J, Hendorfer G, Schoisswohl M, Palmetshofer L and Jantsch W 1994 *Mat. Sci. Forum* **143–7** 715

[21] Löbe K and Boyn R 1988 *Phys. Status Solidi* b **150** 191

[22] Kingsley J D and Aven M 1967 *Phys. Rev.* **155** 235

[23] Ranon U and Low 1963 *Phys. Rev.* **32** 1609

[24] Abragam A and Bleaney B 1970 *Electron Paramagnetic Resonance of Transition Ions* (Oxford: Clarendon)

[25] Buch T, Clerjaud B, Lambert B and Kovacs P 1973 *Phys. Rev.* B **7** 184